



**HAL**  
open science

## Selenium(VI) and copper(II) adsorption using polyethyleneimine-based resins: Effect of glutaraldehyde crosslinking and storage condition

Shengye Wang, Ke Xiao, Yayuan Mo, Bo Yang, Thierry Vincent, Catherine Faur, Eric Guibal

### ► To cite this version:

Shengye Wang, Ke Xiao, Yayuan Mo, Bo Yang, Thierry Vincent, et al.. Selenium(VI) and copper(II) adsorption using polyethyleneimine-based resins: Effect of glutaraldehyde crosslinking and storage condition. *Journal of Hazardous Materials*, 2020, 386, pp.121637. 10.1016/j.jhazmat.2019.121637 . hal-02456548

**HAL Id: hal-02456548**

<https://imt-mines-ales.hal.science/hal-02456548v1>

Submitted on 23 May 2022

**HAL** is a multi-disciplinary open access archive for the deposit and dissemination of scientific research documents, whether they are published or not. The documents may come from teaching and research institutions in France or abroad, or from public or private research centers.

L'archive ouverte pluridisciplinaire **HAL**, est destinée au dépôt et à la diffusion de documents scientifiques de niveau recherche, publiés ou non, émanant des établissements d'enseignement et de recherche français ou étrangers, des laboratoires publics ou privés.

# Selenium(VI) and copper(II) adsorption using polyethyleneimine-based resins: Effect of glutaraldehyde crosslinking and storage condition

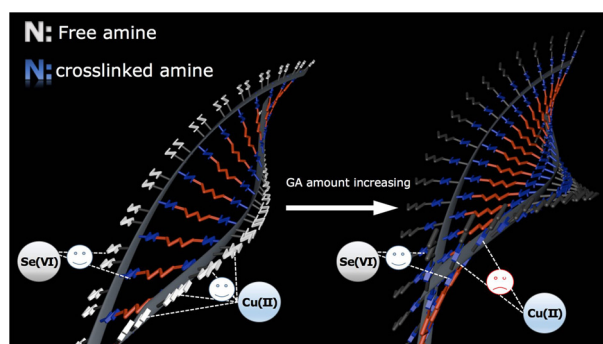
Shengye Wang<sup>a,b</sup>, Ke Xiao<sup>a</sup>, Yayuan Mo<sup>b</sup>, Bo Yang<sup>a,\*</sup>, Thierry Vincent<sup>b</sup>, Catherine Faur<sup>c</sup>, Eric Guibal<sup>b</sup>

<sup>a</sup> College of Chemistry and Environmental Engineering, Shenzhen University, Shenzhen 518060, China

<sup>b</sup> C2MA, IMT Mines Ales, Univ Montpellier, Ales, France

<sup>c</sup> IEM, Institut Européen des membranes, Univ Montpellier, CNRS, ENSCM, Montpellier, France

## GRAPHICAL ABSTRACT



**Keywords:**  
PEI crosslinking  
Se(VI)  
Cu(II)  
Storage  
Stability

## ABSTRACT

This study synthesizes polyethyleneimine-glutaraldehyde (PEI-GA) resins using different amounts of GA to crosslink with a certain amount of PEI and compares these adsorbents for the adsorption of Cu(II) (cations) and Se(VI) (anions). Moreover, the stability of adsorption affinity of PEI-GA resins stored in open or sealed conditions is also studied. Results show that the amount of GA for PEI crosslinking does not affect the adsorption performance for Se(VI), especially when PEI/GA mass ratio is less than 2, while for Cu(II), the increase on GA amount decreases Cu(II) adsorption capacity. This difference is directly correlated to the change in the adsorption mechanism from electrostatic attraction to chelation. The primary and secondary amine groups on PEI can easily react with CO<sub>2</sub> in the air to form carbamate, potentially affecting the adsorption performance of PEI. Results also indicate that the adsorption efficiency for Se(VI) is hardly affected by the storage condition, while that for Cu(II) decreases significantly after 20-day storage compared to the freshly prepared ones. In addition, all of the adsorbents can selectively remove Se(VI) from Se(VI)-As(V) system and Cu(II) from Pb(II)-Cu(II) system, indicating that the crosslinking has no significant influence on the selectivity.

\* Corresponding author.

E-mail address: [boyang@szu.edu.cn](mailto:boyang@szu.edu.cn) (B. Yang).

## 1. Introduction

Amine-rich adsorbents present high adsorption affinity towards both anions and cations in aqueous solutions *via* different mechanisms. Owing to the presence of primary (1/4), secondary (2/4), and tertiary amine (1/4) groups, branched polyethylenimine (PEI)-based materials are continuously being developed for the removal of aqueous contaminants including anions such as chromate, palladium-chloro complexes, and platinum-chloro complex through electrostatic attraction at low pH or metal cations such as copper, lead, and zinc through coordination/chelation onto free amine groups. However, limited by its high solubility in water, PEI has to be immobilized before application. Glutaraldehyde (GA) has been extensively used to immobilize/crosslink PEI through the reaction between primary amine groups of PEI and GA, forming “Schiff’s base” (Hu et al., 2019). Lindén et al. (Lindén et al., 2016) reported that GA crosslinking significantly improved the mechanical and chemical stability of PEI coatings that formed on silica surfaces. PEI-GA resins reported by Kaur et al. Kaur et al. (2018) showed excellent selectivity for Cu(II) binding and metal recovery from complex solutions. But excessive crosslinking will inevitably reduce the number of available primary amine groups and thus decrease the binding properties of PEI (Ghoul et al., 2003). Although many studies regarding the modification of materials using PEI followed by GA or the direct use of PEI-GA resins for the removal of aqueous contaminants have been published previously (Li et al., 2018; Wang et al., 2019), information is lacking on how much GA crosslinking impacts the binding towards different metals onto PEI.

The removal of copper (Cu) and selenium (Se) has attracted attention because these metals represent health hazards for living organisms. The U.S. Environmental Protection Agency (EPA) mandated a maximum acceptable level for Se in drinking water of  $0.05 \text{ mg L}^{-1}$  while for Cu the limit was set to  $1.3 \text{ mg L}^{-1}$ . Selenium can occur in both organic and inorganic forms (including different oxidation states with different toxicities). Due to their high solubility and bioavailability, the inorganic species, selenite and selenate anions, are the dominant species in natural water (Fukushi et al., 2019). Though both anions could bioaccumulate in organisms, selenate is more difficult to remove due to its more stable structure in aqueous solutions than selenite (Hansen et al., 2019). In the case of Cu, free aqueous Cu(II) is the dominant species in acidic solutions. Therefore, Cu(II) can react with the amino groups of the PEI-GA through coordination, and the Se(VI) anions can be retained through the electrostatic attraction when nitrogen atoms are protonated in acidic solutions. However, it is well-known that metal (cations)-nitrogen bonds are inherently weaker on tertiary amine groups than on primary or secondary amine groups (Cotton and Wilkinson, 1988). Therefore, understanding the effect of GA crosslinking, which consumes primary amine groups, on the adsorption performance of PEI for Cu(II) cations is of importance. Moreover, its impact on selenate (anions) binding is also worthy studying. Because these two contaminants can represent a variety of ions in aqueous solutions such as oxoanions or metal complex anions and metal cations, respectively. In addition, primary and secondary amine groups are reported to be unstable when exposed to air as they can easily react with  $\text{CO}_2/\text{H}_2\text{O}$ . Therefore, when stored in open condition for a certain time, the conversion of amine groups to carbamate and/or bicarbonate occurs (Vinodh et al., 2018), which might have detrimental, beneficial or minimal effects on the adsorption performance of PEI towards aqueous contaminants. However, to our knowledge, neither of the effects of crosslinking or the storage conditions on the adsorption properties of PEI-based materials has been studied so far.

This study investigates the effect of different levels of GA crosslinking and storage conditions on the adsorption properties of PEI-GA resins for Se(VI) (selenate anions) and Cu(II) (cations). Moreover, copper is commonly associated with lead in the wastewater from manufacture of printed circuit boards, battery, etc. (Liu et al., 2008), while selenium can coexist with arsenic in the leachates of sedimentary

rocks (Tabelin et al., 2014). Therefore, the selectivity of the adsorbents for Se(VI) in Se(VI)-As(V) system and Cu(II) in Cu(II)-Pb(II) system has been also studied. The results of this study should be useful for the synthesis and storage of various PEI-based or amine-rich adsorbents applied for the removal of aqueous contaminants including anions and cations.

## 2. Materials and methods

### 2.1. Materials

Branched polyethylenimine (PEI, 50 % (w/w) in water), glutaraldehyde (GA, 50 % (w/w) in water), copper nitrate and lead nitrate were purchased from Sigma-Aldrich (Taufkirchen, Germany). Other reagents were supplied by Chem-Lab NV (Zedelgem, Belgium).

### 2.2. Preparation of adsorbents

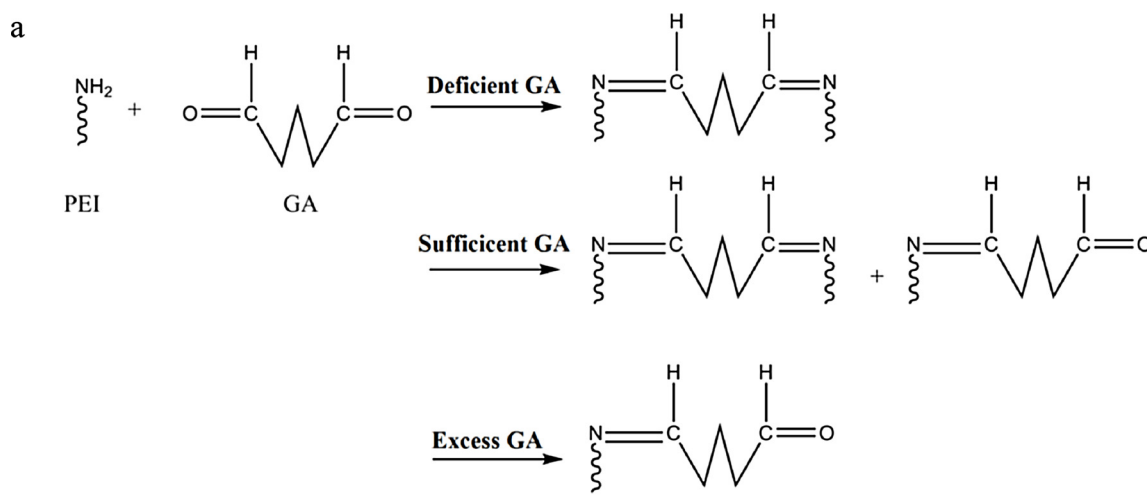
For preparing PEI-GA resins, 40 g of PEI solution (50 %, w/w) were dissolved into 400 ml of pure water. Thereafter, different amounts, namely, 10 g, 16 g, 20 g, and 30 g of GA (50 %, w/w) were added, respectively, under strong agitation ( $\approx 300 \text{ rpm}$ ) of PEI solution for 30 s. The mixtures were sealed and kept at room temperature ( $19^\circ\text{C} - 25^\circ\text{C}$ ) for 16 h to ensure completion of the reaction, which is shown in Fig. 1(a). The reaction can face three different scenarios:

- (1) when there is deficient GA, the crosslinking is formed with one GA molecule and two primary amine groups on PEI;
- (2) when there is excess GA, there is formation of only one Schiff base, with one aldehyde group of GA, the other aldehyde group remains free;
- (3) when GA amount is sufficient, the reaction is between (1) and (2) (co-existence of Schiff base and crosslinked groups).

The obtained PEI-GA resins were thoroughly washed by immersing them in 1 l of deionized water under 50 rpm of agitation for 10 min and filtrated. The washing step was repeated 5 times for each sample. The solids were then freeze-dried at  $-52^\circ\text{C}/0.1 \text{ mbar}$ , for two days, ground to pass through 0.25-mm screen (Retsch, ZM 200, Retsch Technology, Haan, Germany) and stored in seal-packaging by plastic films or in open condition under room atmosphere with a temperature range of  $19^\circ\text{C} - 25^\circ\text{C}$  and relative humidity of 36 %–48 %. The obtained adsorbents prepared using 10 g, 16 g, 20 g, and 30 g of GA are marked as PEI-GA1, PEI-GA2, PEI-GA3 and PEI-GA4, respectively. Fig. 1(b) shows that with the increase of GA amount applied for crosslinking from 10 g to 30 g, the color of the resins turned from yellow to orange-red. Moreover, different storage condition resulted in different colors of the resins after 20 days. The experiment below will show if the storage condition affects their adsorption for Se(VI) and Cu(II). The yield of conversion was calculated based on the mass of obtained resin (i.e.,  $m_{\text{PEI-GA}}$ ) divided by the mass of the PEI and GA introduced for resin preparation (i.e.,  $m_{\text{PEI}} + m_{\text{GA}}$ ). Taking PEI-GA1 as an example, the mass of PEI and GA used for adsorbent preparation was 20.00 g and 5.00 g, respectively, while that of the obtained resins after freeze-drying was 12.11 g. The yield equaled to  $12.11/(20 + 5) \times 100 = 48.4 \%$ . The synthesis process was repeated to obtain freshly prepared materials. Average values and standard deviations (SD) were calculated, which turned out to be  $48.0 \pm 3.8 \%$  for PEI-GA1,  $56.7 \pm 3.1 \%$  for PEI-GA2,  $62.5 \pm 1.9 \%$  for PEI-GA3 and  $72.0 \pm 0.8 \%$  for PEI-GA4.

### 2.3. Characterization of materials

For characterization, freshly resins were prepared and stored in sealed condition before being analyzed within 5 days. Se(VI)-loaded resins were prepared by contacting 0.5 l of  $0.5 \text{ mmol L}^{-1}$  Se(VI) solution with 100 mg of resins for 600 min, while Cu(II)-loaded ones were



Note:

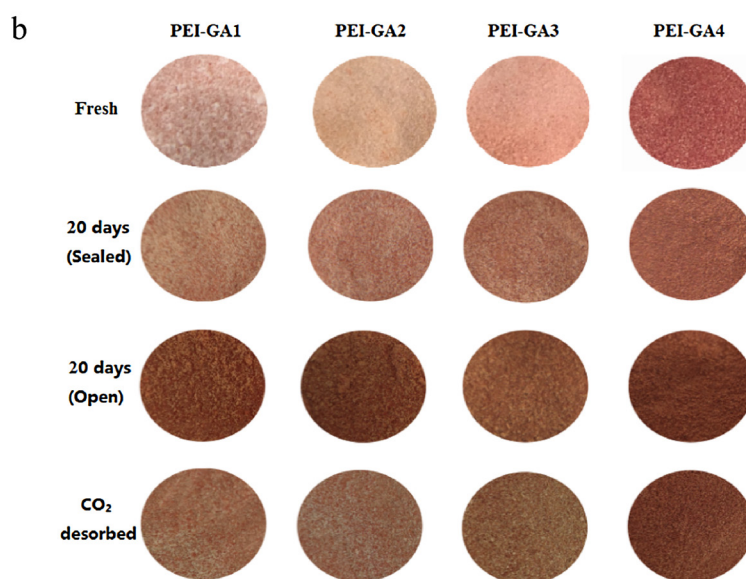
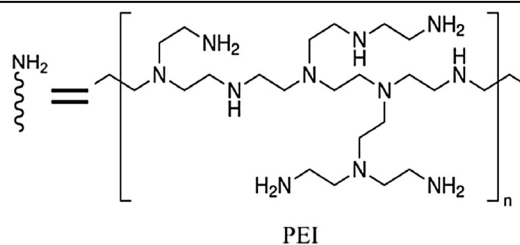


Fig. 1. (a) The reaction of PEI with GA; (b) Images of PEI-GA resins under different conditions.

obtained by contacting 0.51 of 1.0 mmol L<sup>-1</sup> Cu(II) solution with 200 mg of resins for 48 h. Those contaminant-loaded adsorbents were freeze-dried at -52 °C/0.1 mbar for 24 h and stored in sealed condition before being characterized.

Elemental analyses were carried out with an Elementar Vario EL cube (Hanau, Germany).

FT-IR spectrometry analysis was performed in the range 4000–400 cm<sup>-1</sup> using an FTIR-ATR (Attenuated Total Reflectance tool) Bruker VERTEX70 spectrometer (Bruker, Ettlingen, Germany).

X-ray photoelectron spectroscopy (XPS) measurements were carried out with a K-Alpha + spectrometer (ThermoFisher Scientific, East Grinstead, UK).

Scanning electron microscopy (SEM) was performed using an environmental scanning electron microscope Quanta FEG 200 (FEI

France, Thermo Fisher Scientific, Mérégnac, France).

The pH<sub>PZC</sub> values of PEI-GA resins that are freshly prepared or stored in open condition after 20 days were measured using the pH-drift method. Briefly, 50 ml of 0.1 M NaCl solution with initial pH (pH<sub>0</sub>) range of 5–12 were mixed with 0.1 g of the adsorbent for 48 h under agitation with a speed of 150 rpm at room temperature. Thereafter, final pH (pH<sub>f</sub>) was measured and plotted against pH<sub>0</sub>. The values of pH<sub>PZC</sub> correspond to the point at which pH<sub>f</sub> was equal to pH<sub>0</sub>.

#### 2.4. Adsorption experiments

The adsorption experiments were carried out by contact of a given amount of adsorbents (m, g) with a given volume (V, L) of metal-containing solution (C<sub>0</sub>, mg L<sup>-1</sup>) at room temperature with a range of

16 °C – 25 °C. At desired time intervals, 2 ml of samples were collected, filtrated and analyzed using inductively coupled plasma atomic emission spectrometry (ICP-AES, JY Activa M, Jobin-Yvon, Horiba, Longjumeau, France). It is noted that unless otherwise specified, all the adsorbents used were those freshly prepared and stored in sealed condition less than 10 days.

For the different experimental series, the conditions were different and the full experimental details are reported in the caption of each figure. Detailed information can be found in Supplementary Materials (SM).

## 2.5. Modeling and selectivity

### 2.5.1. Modeling

Uptake kinetics has been modeled using the pseudo-first order rate equation (PFORE, Eq. 1) and the pseudo-second order rate equation (PSORE, Eq. 2).

$$q_t = q_{eq}(1 - e^{-k_1 t}) \quad (1)$$

$$q_t = \frac{q_{eq}^2 k_2 t}{1 + q_{eq} k_2 t} \quad (2)$$

where  $q_t$  and  $q_{eq}$  ( $\text{mmol g}^{-1}$ ) are the adsorption capacities adsorbed at  $t$  and at equilibrium, respectively. The parameters  $k_1$  and  $k_2$  are the apparent rate constants of PFORE ( $\text{min}^{-1}$ ), and PSORE ( $\text{g mmol}^{-1} \text{min}^{-1}$ ), respectively.

Sorption isotherms represent the solute distribution at equilibrium between the liquid and the solid phase for different initial metal concentrations: the adsorption capacity ( $q$ ) is plotted vs. the residual metal concentration ( $C_{eq}$ ). One of the most commonly used models for describing solute adsorption to soils is the Langmuir model (Eq. 3).

$$q_{eq} = \frac{K q_m C_{eq}}{1 + K C_{eq}} \quad (3)$$

where  $q_m$  and  $K$  are the Langmuir parameters corresponding to the adsorption capacity at saturation of the monolayer ( $\text{mmol g}^{-1}$ ) and  $K$  is the affinity coefficient ( $\text{L mmol}^{-1}$ ).

The parameters were obtained by non-linear regression analysis using Origin 9.0 (Origin software Inc., San Clemente, CA, USA).

### 2.5.2. Selectivity

The separation factor ( $\alpha_{i/j}$ ,  $i$  and  $j$  referring to co-existing contaminants in binary system) is calculated for defining the possible preference of the adsorbent for a given contaminant in the binary adsorption system by the following equation:

$$\alpha_{i/j} = \frac{q_{eq,i} C_{eq,j}}{q_{eq,j} C_{eq,i}} \quad (4)$$

If  $\alpha_{i/j} > 1$ ,  $i$  is preferred; alternatively,  $j$  is preferred.

## 3. Results and discussion

### 3.1. Characterization

#### 3.1.1. SEM and elemental analysis

Fig. 2 shows the SEM images of PEI-GA adsorbents. It is noted that all the adsorbents were crushed to pass a 0.25-mm screen using a Retsch ZM 200 centrifugal mill. Generally, the adsorbents consist of small particles with a size less than 0.2 mm; however, some aggregation of these small particles are observed for all the adsorbents, except for PEI-GA4. The aggregation is probably due to the hydrogen-bonding interactions between amine groups, especially primary amines, that gathers the tiny particles. This is the first clue that most of primary amine groups have been consumed by GA in PEI-GA4.

The SEM images and elemental maps for N, Se and Cu of Se(VI)-

loaded and Cu(II)-loaded resins are shown in Figs. S1 and S2 (see Supplementary Materials, SM). After sorption, much less aggregates are found from SEM images. This is because that most amine groups are protonated after interacting with acidic contaminant solutions, resulting in the electrostatic repulsion which separates those aggregated particles. Moreover, N distribution is roughly homogeneous in the whole mass of the adsorbents. This means the resins are homogeneous and PEI is uniformly dispersed. The distribution of Se or Cu is clearly correlated to that of N, suggesting that N plays an important role in binding Se(VI) and Cu(II).

Based on the elemental composition of PEI and GA, the elemental composition of PEI-GA resins only consists of C, H, O and N. Elemental analysis (Table 1) shows that for raw samples, C content increases with increasing GA amount, while an opposite trend is found for N content. For PEI-GA1, GA amount is deficient, resulting in a large amount of PEI loss; the yield of conversion is the lowest among the four adsorbents. Therefore, its N content is only slightly higher than that of other samples. However, for PEI-GA4, there is an excess of GA; therefore, one Schiff base is formed with one aldehyde group of the GA and the other aldehyde group remains free. In this case, GA takes a larger part in the final product compared to the other three adsorbents, leading to a lower N content. When there is deficient GA, the crosslinking is formed with one GA molecule and two primary amine groups on PEI, meaning that, in this case (for example, PEI-GA1), no oxygen should be found. Surprisingly, O element can be found in the four adsorbents. This could be attributed to the eventual capture of  $\text{CO}_2$  and  $\text{H}_2\text{O}$  (when the air is humid) during the synthesis. Fig. S3 (see SM) shows the proposed reactions between PEI and  $\text{CO}_2$  and  $\text{H}_2\text{O}$ . After storing in open condition for 20 days, a very small decrease on N content is observed; this is due to the capture of with  $\text{CO}_2$  and  $\text{H}_2\text{O}$  (or their reaction), increasing the mass of the adsorbents and thus reducing the proportion of N content. After  $\text{CO}_2$  desorption process, the content of C, N and O increases/or decreases back towards the original values, indicating that the changes during storage are mostly reversible. It is worth studying how this change affects the binding properties of these adsorbents for Cu(II) and Se(VI).

#### 3.1.2. FTIR

The functional groups present on the adsorbents can be identified using FTIR spectroscopy. Moreover, by comparing the spectra before and after adsorption of contaminants, it is possible to explain the mechanisms of the adsorption process through the identification of functional groups involved in metal binding. The corresponding FTIR spectra of the freshly prepared and contaminant-loaded adsorbents and those after 20-day storage and  $\text{CO}_2$  desorption process are shown in Fig. 3. The assignments of the main bands in spectra are reported in Tables S1–S4 (see SM). The tables show that contaminant-free spectra of the four freshly prepared adsorbents present very similar profiles. Taking PEI-GA1 as an example, the broad absorption peaks observed between  $3500\text{--}3000 \text{ cm}^{-1}$  corresponds to the overlapping of  $-\text{OH}$  and  $-\text{NH}$  peaks (Sun et al., 2011). The peaks at  $2928$  and  $2812 \text{ cm}^{-1}$  represent  $\text{CH-}$  stretching vibrations of  $\text{CH}_2$  and  $\text{CH}$  groups, respectively (Kuila et al., 2012). The peak at  $1655 \text{ cm}^{-1}$  is due to the formation of  $\text{C=N}$  bonds (Li et al., 2019), indicating that crosslinking has taken place between primary amine groups of PEI and GA, forming “Schiff’s base” (Hu et al., 2019). The peak at  $1570 \text{ cm}^{-1}$  can be assigned to the  $\text{NH-}$  bending vibration of primary amines (Zhang et al., 2018). It is noteworthy that, in the figures, the intensity of this peak becomes less and less noticeable as the GA amount increases and almost disappears for PEI-GA4, suggesting that GA crosslinks most of the primary amine groups on PEI-GA4. Besides, peaks at  $1458$  and  $1281 \text{ cm}^{-1}$  correspond to  $\text{CH-}$  bending vibration (Sharifi et al., 2019). Peaks at  $1102$  and  $1053 \text{ cm}^{-1}$  are assigned to  $\text{CO-}$  asymmetric stretching (Ren et al., 2017). The  $\text{CO-}$  peaks should not be found in the raw adsorbents, since the molecular formula of PEI-GA does not have  $\text{CO-}$  bond, unless it is contaminated. As discussed above, PEI could react with  $\text{CO}_2$  and has

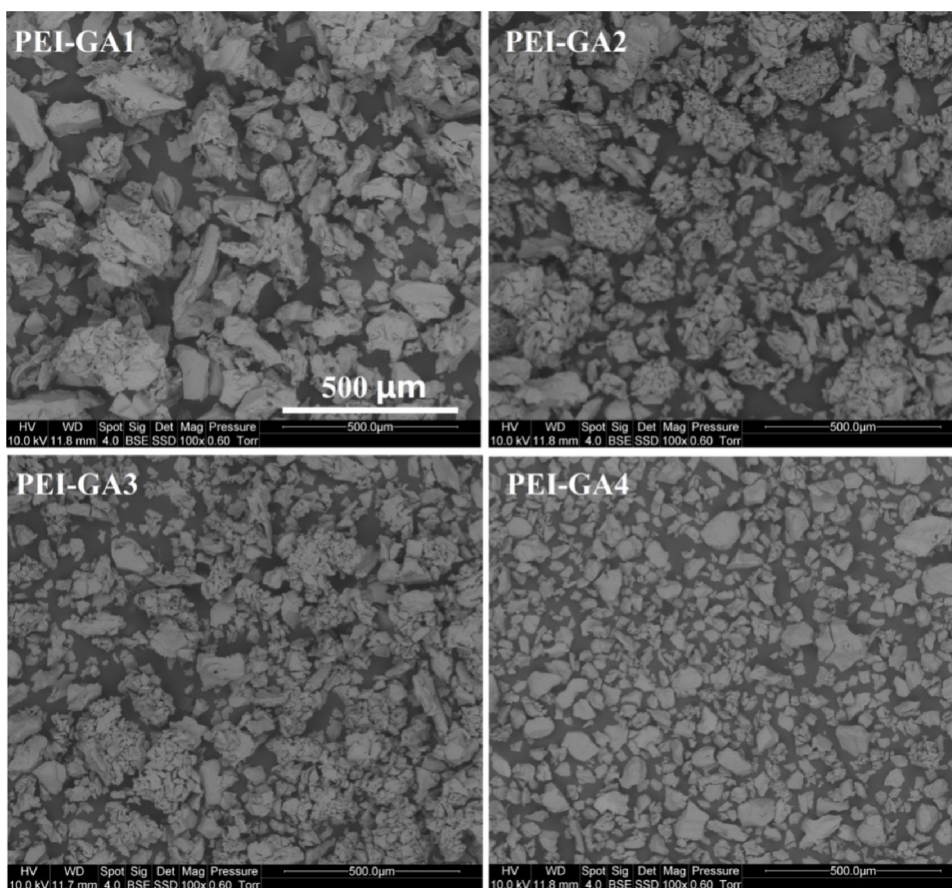


Fig. 2. SEM images of the PEI-GA resins.

**Table 1**  
Elemental analysis of PEI-GA adsorbents (wt.%).

Element	Condition	PEI-GA1	PEI-GA2	PEI-GA3	PEI-G4
C	Freshly prepared	62.13 ± 1.22	61.03 ± 0.64	61.27 ± 0.70	63.41 ± 0.83
	After 20 days <sup>a</sup>	53.79 ± 0.39	52.40 ± 0.58	51.20 ± 1.08	54.75 ± 0.86
	After desorption step	59.75 ± 2.00	60.18 ± 0.08	61.00 ± 0.19	61.87 ± 0.85
N	Freshly prepared	22.67 ± 0.85	22.27 ± 0.52	21.20 ± 1.18	18.41 ± 0.48
	After 20 days	21.89 ± 1.06	20.91 ± 1.05	20.66 ± 1.37	17.2 ± 1.24
	After desorption step	22.10 ± 0.53	22.07 ± 0.80	21.45 ± 1.09	18.10 ± 1.06
O	Freshly prepared	4.06 ± 1.52	6.02 ± 0.15	7.12 ± 0.09	8.34 ± 0.03
	After 20 days	14.54 ± 1.14	17.28 ± 1.64	19.00 ± 0.08	18.75 ± 1.97
	After desorption step	7.91 ± 1.75	7.41 ± 0.92	6.98 ± 0.35	10.42 ± 2.74
H	Freshly prepared	11.14 ± 0.25	10.69 ± 0.28	10.42 ± 0.56	9.85 ± 0.38
	After 20 days	9.78 ± 0.46	9.41 ± 0.02	9.14 ± 0.21	9.31 ± 0.13
	After desorption step	10.25 ± 0.28	10.35 ± 0.20	10.57 ± 1.25	9.60 ± 0.81

<sup>a</sup>: in open condition.

been reported to be high-capacity adsorbent for CO<sub>2</sub> capture (Xu et al., 2002). The result here is a second evidence that the adsorbents partially react with CO<sub>2</sub> and/or H<sub>2</sub>O during preparing process. For both primary and secondary amines, the adsorption of CO<sub>2</sub> involves hydrogen bonding with surface silanols or neighboring alkylamines, possibly through various arrangements upon the formation of carbamic acid. After storing in open condition for 20 days, taking PEI-GA1 samples as an example (shown in Fig. 3d), the intensity of peak at 1570 cm<sup>-1</sup> corresponding to NH<sub>2</sub> bending vibration of primary amines decreases slightly, while the peak at around 1655 cm<sup>-1</sup> becomes much wider. This can be due to the overlapping of COO<sup>-</sup> stretching at 1610 cm<sup>-1</sup> (Sanchez-Ballester et al., 2019). These results indicate the formation of COO<sup>-</sup> groups by the reaction of free amine groups with CO<sub>2</sub>. The same trend is also found for the other adsorbents (shown in Figure S4). After a thermal treatment under nitrogen atmosphere, the peak at 1655 cm<sup>-1</sup>

red-shifts and becomes less wide compared to resins stored after 20 days. This might be due to the disappearance of COO<sup>-</sup> groups. The contamination could affect the adsorption properties of PEI-GA for metal adsorption, which will be discussed below.

After Cu(II) binding, the band around 1570 cm<sup>-1</sup> specific to primary amine groups completely disappears. This significant change confirms the involvement of NH<sub>2</sub> of primary amines groups in Cu(II) adsorption onto the adsorbents. Other changes are associated to slight shifts of the bands. Taking PEI-GA1 as an example, the bands shift at 3261, 2928, 1655 and 1053 cm<sup>-1</sup>, which are ascribed to the stretching vibrations of NH<sub>2</sub> (Kiruba et al., 2018), CH<sub>2</sub> (Kuila et al., 2012), C=N (Li et al., 2019) and CO (Ren et al., 2017), respectively. The disappearance of peaks at 2812 and 1102 cm<sup>-1</sup>, corresponding to C-H stretching and CO stretching, respectively, was also observed. This could be due to the reaction of carbamate with H<sub>2</sub>O in humid condition

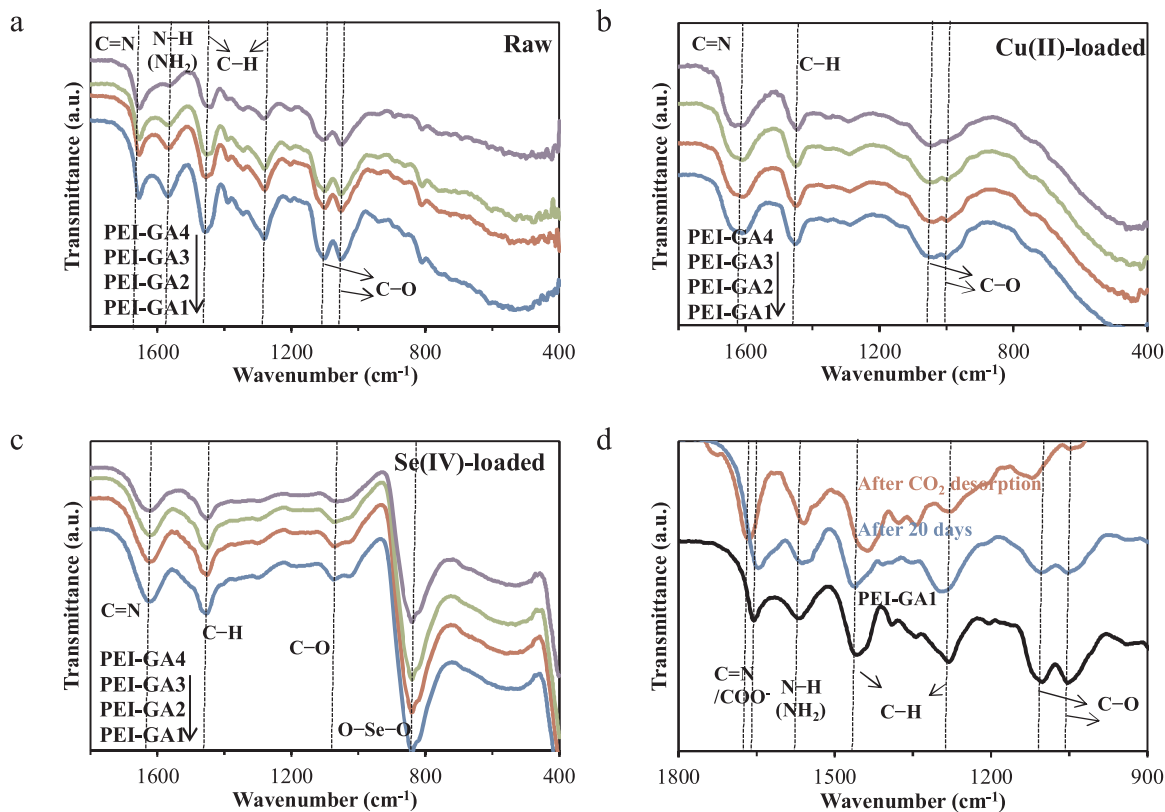


Fig. 3. FTIR spectra of (a) raw PEI-GA, (b) and (c) before and after Cu(II) and Se(VI) adsorption and (d) PEI-GA1 after 20 days of storage and after CO<sub>2</sub> desorption process.

to form bicarbonate or carbamic acid (Wijesiri et al., 2019).

In the case of the Se(VI)-adsorbed samples, a new peak at 840 cm<sup>-1</sup>, assigned to the vibrations of SeO<sub>3</sub> pyramidal groups with C3v point symmetry (Bachvarova et al., 2005), appears regardless of adsorbents, confirming the binding of SeO<sub>4</sub><sup>2-</sup>. In addition, the stretching of C=N is shifted toward lower wavenumbers. Other changes consist of the disappearance of peaks corresponding to NH- bending vibration of primary amines, CH- bending and asymmetric stretching vibration of C-OC-.

In addition, the pH<sub>PZC</sub> of freshly prepared PEI-GA1, PEI-GA2, PEI-GA3 and PEI-GA4 are 9.95, 10.11, 9.80 and 9.69, respectively. After 20-day storage, these values decreased to 9.54, 9.72, 9.46 and 9.43, respectively. This decrease on pH<sub>PZC</sub> values are probably due to the formation of groups with a lower pK<sub>a</sub> value, further (besides the result of FTIR) confirming the formation of COO<sup>-</sup> groups, whose pK<sub>a</sub> value is close to 4. The experiments below (see section 3.3) will discuss how this change affects the adsorption properties of the resins for Cu(II) and Se(VI).

### 3.1.3. XPS

To further confirm the contamination of PEI-GA resins when stored in open condition for a certain time, XPS was used to investigate surface composition of PEI-GA resins before and after exposure to the air after 20 days. As expected, XPS of freshly prepared materials (Fig. 4a) reveals the presence of N, C and O. The N 1s peak is broad and can be resolved into two components: (a) a high binding energy (399 eV) attributed to amine or amide groups and (b) a lower binding energy one (398.9 eV) assigned to the N in the tertiary amine groups (> N-) (Ma et al., 2014). The amount of tertiary amine groups increases with the increasing GA amount, due to the reaction between aldehyde groups on GA and free amine groups on PEI. The binding energy around 284.8 eV and 285.8 eV could be due to C-C bond and CN or COC- bond, respectively (Wang et al., 2019). The contribution at around

287.3–280.0 eV represents C=O functions, which could be attributed to uncrosslinked aldehyde groups of GA or a slight adsorption of CO<sub>2</sub> because of the presence of abundant free amine groups during preparation process.

After 20-day storage in open condition, new peaks, shown in Fig. 4b, appear at around 288.1 eV for C 1s representative for carboxylate and 402.1 eV for N 1s due to protonated nitrogen associated with the formation of the carbamate ion. These peaks firmly confirm the interaction of CO<sub>2</sub> and PEI-GA resins.

### 3.2. Effect of pH on adsorption kinetics

Raw wastewaters containing Cu(II) or Se(VI) are commonly acidic, such as Cu(II) in printed circuit board wastewater (pH 1) (Chou et al., 2015), mix electroplating wastewater (pH 1.6) (Kul and Oskay, 2015), and smelter wastewater (pH < 1) (Hansen et al., 2015). To ensure no formation of metal hydroxide precipitates and avoid using too much pH-adjusting reagents such as NaOH, CaO, etc. when applied practically, the effect of pH was conducted in acidic condition with the pH range of 2–3. Fig. 5 shows the effect of pH on Se(VI) and Cu(II) adsorption kinetics. In general, the adsorption of Se(VI) presents an anionic behavior, slightly decreasing as the pH increased from 2 to 3. The trend is attributed to the predominant selenium species in solution and the surface charges of adsorbents. The pK<sub>a</sub> values of primary, secondary, and tertiary amine groups on PEI were reported as 4.5, 6.7, and 11.6, respectively (Willner et al., 1993). The pH<sub>PZC</sub> (Table S5, see SM) of the resins is in the range of 9.69 to 10.11. Since the initial pH range of the present study is between 2.0 and 3.0 (corresponding to final pH between 2.1–4.3), the reactive groups are strongly protonated. These protonated groups can only bind anionic species. Therefore, as is shown in Fig. S5, the adsorption decreases as the percentage of the aqueous species HSeO<sub>4</sub><sup>-</sup> decreases. Erosa et al. (Erosa et al., 2009) observed a gradual decrease on Se(VI) adsorption as pH increased from 2 to 10

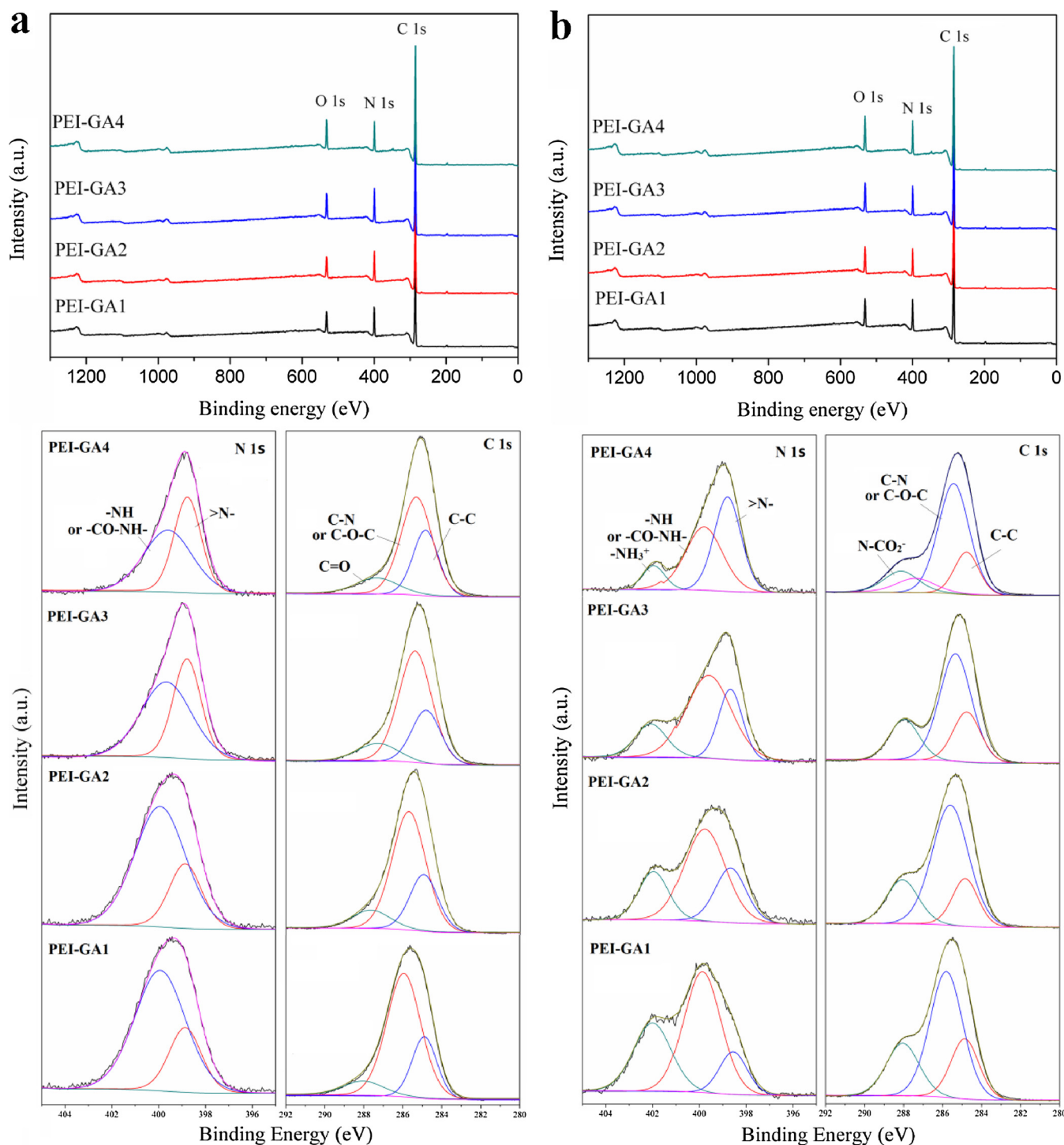


Fig. 4. X-ray photoelectron spectra of PEI-GA resins (a) freshly prepared and (b) after 20-day storage in open condition.

using weakly basic anion exchangers that possess primary, secondary and/or tertiary amino groups. This decrease on Se(VI) binding was due to the decline on the degree of amine protonation and the decrease of the fraction of  $\text{HSeO}_4^-$ . Similarly, Yamani et al. [Yamani et al. \(2014\)](#) reported that the adsorption of Se(VI) onto chitosan-based beads decreased at alkaline pH. The difference of Se(VI) adsorption among the adsorbents is negligible, especially among PEI-GA1, PEI-GA2 and PEI-GA3. The level of GA crosslinking for PEI causes different contents of primary amine groups in the adsorbents, but does not affect significantly the total amount of amine groups (or N content), except for PEI-GA4 (confirmed by elemental analysis). Therefore, the lowest Se

(VI) adsorption capacities of PEI-GA4 can be directly explained by the lower N content compared with the other adsorbents.

The trend found for Cu(II) cations is completely opposite: the adsorption efficiency is strongly affected by solution pH. Negligible adsorption is found when initial pH value is 2.0 and the adsorption efficiency increases significantly when initial pH increases to 3.0, corresponding to equilibrium pH value of 3.63 for PEI-GA1, 3.64 for PEI-GA2, 3.59 for PEI-GA3 and 3.42 for PEI-GA4. The amine groups on the adsorbents are fully protonated in all solutions within selected pH range, resulting in the electrostatic repulsion of Cu(II). As pH increases, this electrostatic repulsion reduces, leading to better adsorption



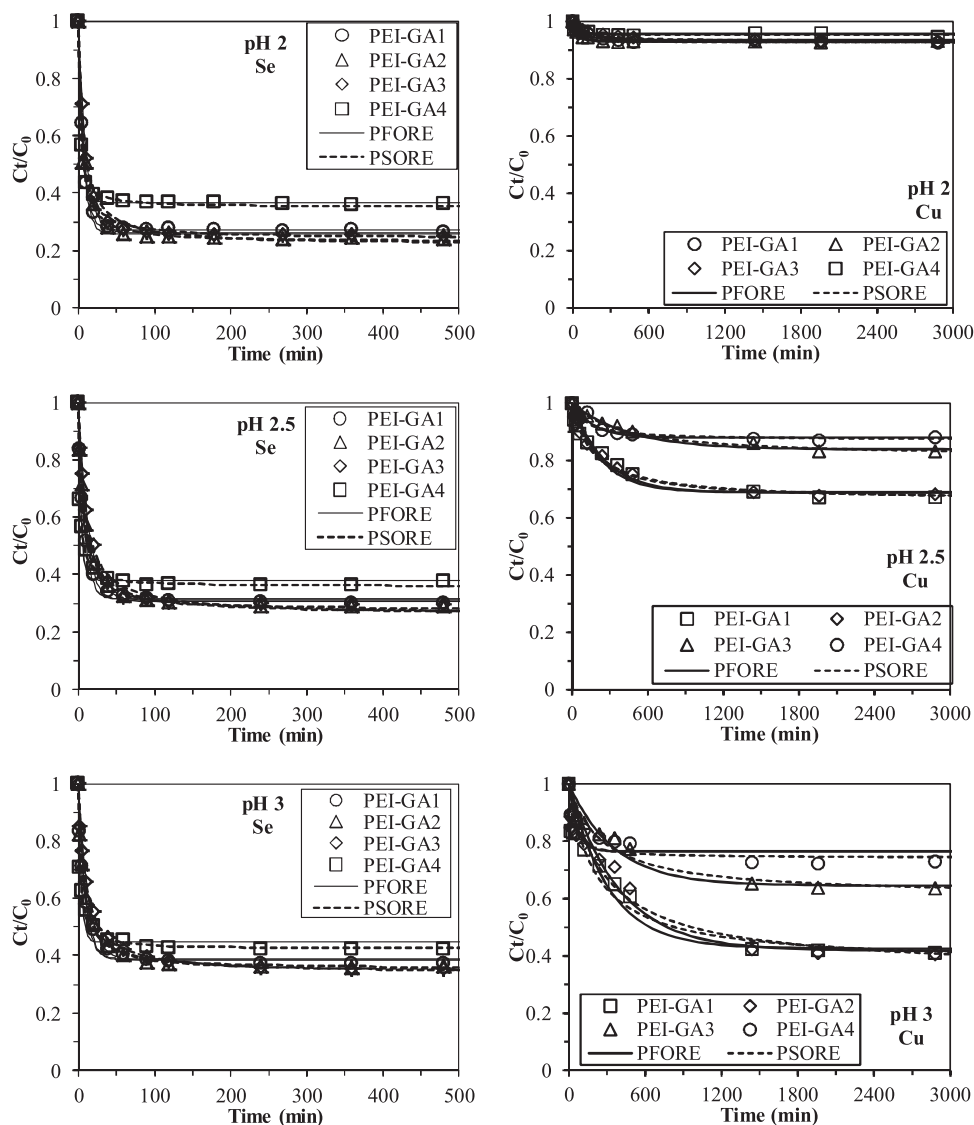


Fig. 5. Effect of pH on Se(VI) and Cu(II) adsorption-kinetics modeling using PFORE and PSORE (Volume: 0.5 L; Adsorbent mass: 100 mg for Se(VI) and 200 mg for Cu(II); Room temperature (19–25 °C);  $C_0$ : 0.5 mmol L<sup>-1</sup> for Se(VI) and 1 mmol L<sup>-1</sup> for Cu(II)).

performance. The main adsorption interaction can be summarized as the coordination bonding between Cu(II) and primary and secondary amine groups on PEI-GA. The binding potential of tertiary amine groups on the adsorbents is limited due to the lower stability constants of complexes with tertiary amines than those with primary or secondary amines (Baldwin et al., 1983). The amount of primary amine groups on the adsorbents decreases gradually as the level of crosslinking between PEI and GA increases. This can explain the big gap of the adsorption efficiency among PEI-GA2, PEI-GA3 and PEI-GA4. Interestingly, apart from the first 10 h of reaction, the equilibrium adsorption efficiencies of PEI-GA1 and PEI-GA2 are almost the same. This could be due to that the amount of GA added for crosslinking for PEI-GA1 is not enough and a certain amount of PEI is not crosslinked or well immobilized; therefore, during washing step, some free PEI may be released and thus the adsorption capacity is not as high as it is expected.

The pseudo-second order rate equation (PSORE) and the pseudo-first order rate equation (PFORE) were used to fit experimental data. The plots shown in Fig. 5 indicate that both PFORE and PSORE can be used to fit kinetic profiles. However, the parameters shown in Table 2 for Cu(II) and Table 3 for Se(VI) suggest that the PSORE fits the data slightly better with all the values of determination coefficient ( $r^2$ ) more than 0.90. The apparent rate constants  $k_1$  and  $k_2$  of PEI-GA4 for both

Table 2

Kinetics constants for the adsorption of Cu(II) at pH 3.

Models	Parameters	PEI-GA1	PEI-GA2	PEI-GA3	PEI-GA4
PFORE	$q_{eq,exp}$ (mmol L <sup>-1</sup> )	1.33	1.34	0.82	0.61
	$q_{eq,cal}$ (mmol L <sup>-1</sup> )	1.29	1.31	0.80	0.53
	$k_1 \times 10^3$ (min <sup>-1</sup> )	3.2	2.5	2.8	15.6
	$r^2$	0.87	0.87	0.87	0.78
PSORE	$q_{eq,cal}$ (mmol L <sup>-1</sup> )	1.41	1.47	0.89	0.58
	$k_2 \times 10^3$ (g mmol <sup>-1</sup> min <sup>-1</sup> )	3.3	2.3	4.4	5.2
	$r^2$	0.91	0.90	0.91	0.87

Table 3

Kinetics constants for the adsorption of Se(VI) at pH 2.

Models	Parameters	PEI-GA1	PEI-GA2	PEI-GA3	PEI-GA4
PFORE	$q_{eq,exp}$ (mmol L <sup>-1</sup> )	4.69	4.82	4.78	4.12
	$q_{eq,cal}$ (mmol L <sup>-1</sup> )	4.63	4.68	4.69	4.03
	$k_1 \times 10^3$ (min <sup>-1</sup> )	139.8	148.6	98.2	227.6
	$r^2$	0.99	0.95	0.99	0.99
PSORE	$q_{eq,cal}$ (mmol L <sup>-1</sup> )	4.82	4.87	4.95	4.14
	$k_2 \times 10^3$ (g mmol <sup>-1</sup> min <sup>-1</sup> )	50.0	55.1	30.9	117.0
	$r^2$	0.98	0.98	0.99	0.99

contaminants are higher than those for the other three adsorbents; this could be due to poorer mass transfer property caused by the aggregation of PEI-GA1, PEI-GA2 and PEI-GA3 particles, which has been discussed in section 3.1.1.

In order to further confirm the effect of GA crosslinking on adsorption capacities of PEI-GA resins for Se(VI) and Cu(II), adsorption isotherms were conducted at pH 2 for Se(VI) and pH 3 for Cu(II). The results shown in Fig. S6 are in good agreement with those obtained by adsorption kinetics. The maximum adsorption capacity ( $q_m$ ) calculated from Langmuir model of PEI-GA1 for Se(VI) is  $5.25 \text{ mmol g}^{-1}$ , very close to  $5.14 \text{ mmol g}^{-1}$  of PEI-GA2 and  $5.05 \text{ mmol g}^{-1}$  of PEI-GA3 and slightly higher than  $4.24 \text{ mmol g}^{-1}$  of PEI-GA4. However,  $q_m$  of PEI-GA1 and PEI-GA2 for Cu(II) are  $1.57$  and  $1.40 \text{ mmol g}^{-1}$ , respectively, much higher than  $0.87 \text{ mmol g}^{-1}$  of PEI-GA3 and  $0.69 \text{ mmol g}^{-1}$  of PEI-GA4.

### 3.3. Effect of different storage conditions on adsorption capacity

The chemical stability of the functional groups on the adsorbents is essential for further application. When exposed to the air for a long time, the active amine groups on the adsorbents could be converted into carbamate and/or bicarbonate (Vinodh et al., 2018), which might have detrimental, beneficial or minimal effects on their adsorption capacity for aqueous contaminants. The storage stability of the adsorbents was tested by comparing the adsorption capacity of PEI-GA freshly prepared and stored in sealed condition or in open condition after 20 days. Fig. 6 shows that the adsorption efficiency for Se(VI) is hardly affected by the storage conditions. No significant difference is observed between the adsorbents prepared freshly and stored in sealed condition after 20

days; for those stored in open condition, only a slight decrease on adsorption capacity can be found regardless of adsorbent type. This decrease might be caused by the decrease of N content which has been confirmed by elemental analysis. For Cu(II), the adsorption capacity of freshly prepared PEI-GA1, PEI-GA2, PEI-GA3 and PEI-GA4 is  $1.33$ ,  $1.33$ ,  $0.82$  and  $0.61 \text{ mmol g}^{-1}$ , respectively. After storing in open condition for 20 days, those values decrease significantly to  $1.02$ ,  $0.91$ ,  $0.60$  and  $0.56 \text{ mmol g}^{-1}$ , respectively, while those of the adsorbents stored in sealed condition only decrease to  $1.30$ ,  $1.26$ ,  $0.80$  and  $0.57 \text{ mmol g}^{-1}$ , respectively. The reason causing the decrease on adsorption could probably be that primary and secondary amine groups that are active for Cu(II) adsorption on PEI-GA adsorbents stored in open condition react with  $\text{CO}_2/\text{H}_2\text{O}$  to form carbamate/bicarbonate. Although carbonyl groups can potentially adsorb Cu(II), their adsorption affinity for Cu(II) at pH 3 is intrinsically lower than that of primary and secondary amine groups. Monier et al. (2010) reported a Cu(II) adsorption capacity of  $68 \text{ mg g}^{-1}$  of amine-based adsorbent (chitosan resin) at pH 3. This is much higher than that of carboxyl-based materials under the similar condition, such as  $28 \text{ mg g}^{-1}$  of zirconium oxide immobilized alginate beads (Kwon et al., 2016) and  $10.2 \text{ mg g}^{-1}$  of alginate beads (An et al., 2015). For Se(VI) adsorption, the adsorption is only associated with amount of nitrogen. Thus, it is hardly affected by the formation of carbamate/or bicarbonate, since N content does not change significantly. Another interesting finding is that the adsorption kinetics of all the adsorbents in open condition for Cu(II) is slower than that of sealed ones. Except for PEI-GA4, the other three adsorbents stored under open condition still present a slow growing trend, while those stored in sealed condition already achieve equilibrium at 24 h. However, the reason causing the slower kinetics remains unclear. One

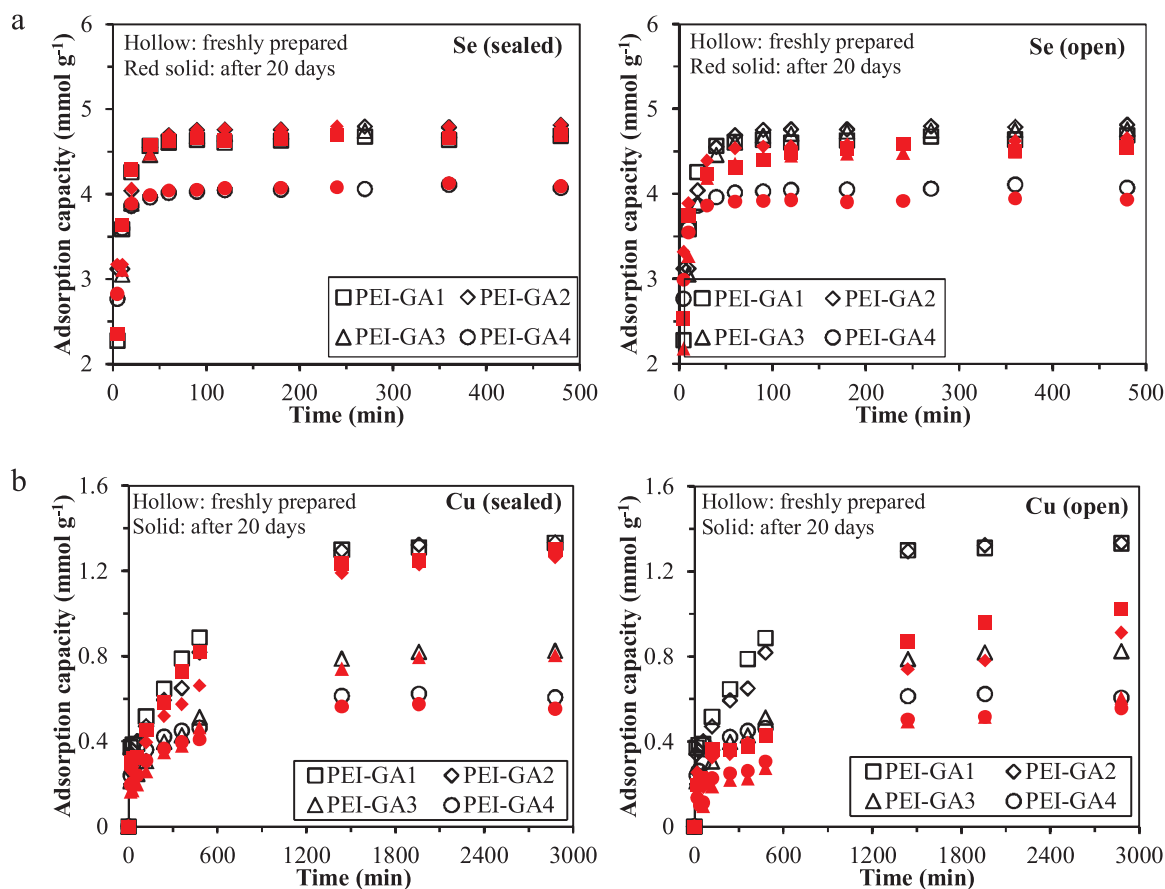


Fig. 6. Effect of storage condition on adsorption capacity of PEI-GA for (a) Se(VI) and (b) Cu(II) (Volume:  $0.5 \text{ L}$ ; Room temperature ( $19 - 25 \text{ }^\circ\text{C}$ ); Adsorbent mass:  $100 \text{ mg}$  for Se(VI) and  $200 \text{ mg}$  for Cu(II);  $C_0$ :  $0.5 \text{ mmol L}^{-1}$  for Se(VI) and  $1 \text{ mmol L}^{-1}$  for Cu(II);  $\text{pH}_0$ : 2 for Se(VI) and 3 for Cu(II)). Note: freshly prepared adsorbents were the materials stored in sealed condition within 5 days.

possibility is that the formation of carbamate/or bicarbonate results in a tighter polymer network which makes it more difficult for contaminants to diffuse to the adsorption sites. To conclude, the results indicate that the storage condition plays an important role on Cu(II) adsorption onto adsorbents containing primary or secondary amine groups.

To confirm whether the decrease on Cu(II) adsorption is caused by CO<sub>2</sub> and if the contamination is reversible. The re-dried, CO<sub>2</sub>-loaded and CO<sub>2</sub>-desorbed adsorbent were compared for Cu(II) adsorption at pH 3. Fig. S7 (see SM) shows that the re-drying process does not recover the adsorption performance significantly, confirming that humidity is not the main cause of decrease on contaminant removal. The adsorbents immersed in pure CO<sub>2</sub> show a sharp decrease Cu(II) adsorption capacities and after the desorption process, the adsorption properties recover significantly. The results further confirm that the decrease on adsorption capacity for Cu(II) is mainly caused by the contamination of CO<sub>2</sub>.

### 3.4. Adsorption in binary system

To investigate the selectivity of PEI-GA adsorbents for Se(VI) and Cu(II), studies are carried out in Se-As and Cu-Pb binary systems, respectively. The results of competitive adsorption of Se(VI) and As(V) from the binary solutions with different pHs are shown in Fig. 7. All the adsorbents have a greater affinity for Se(VI) over As(V) at pH 2. It is also noteworthy that for the three adsorbents, the equilibrium adsorption capacity is only slightly affected by the presence of As(V) at selected pH values (Fig. S8, see SM). Moreover, As(V) is hardly removed along with Se(VI), indicating that all of the adsorbents can selectively remove Se(VI) from Se-As system at pH 2. This can be explained by the limited adsorption performance of these adsorbents for As(V) at pH 2 (Fig. S9, see SM). When solution pH increases to pH 3, the adsorption of As(V) increases, especially for the first 10 min. However, these values decrease dramatically after a longer contact time. This is due to the progressive decrease of available reactive groups and the strong competition between Se(VI) and As(V) for occupying free adsorption sites. Therefore, As(V) ions start to be replaced by Se(VI) and released into the solution. For example, within 10 min, the maximum adsorption capacity of PEI-GA1, PEI-GA2, PEI-GA3 and PEI-GA4 for As(V) reaches 0.67 mmol g<sup>-1</sup>, 0.49 mmol g<sup>-1</sup>, 0.52 mmol g<sup>-1</sup>, and 0.34 mmol g<sup>-1</sup>, respectively. However, these values decrease to 0.40 mmol g<sup>-1</sup>, 0.28 mmol g<sup>-1</sup>, 0.26 mmol g<sup>-1</sup>, and 0.16 mmol g<sup>-1</sup>, respectively, after 360 min of reaction, while those for Se(VI) maintain around 4.01 mmol g<sup>-1</sup>, 4.10 mmol g<sup>-1</sup>, 3.95 mmol g<sup>-1</sup>, and 3.56 mmol g<sup>-1</sup>, respectively. The same phenomenon is observed for Cu(II) and Pb(II) adsorption from binary solutions. The adsorption capacity of Pb(II) in binary system is negligible at pH 2 and pH 2.5, while at pH 3, it reaches 0.21–0.35 mmol g<sup>-1</sup> within the first hour but decreases to less than 0.16 mmol g<sup>-1</sup> after a longer reaction time. The results are also confirmed by separation factors ( $\alpha_{Se/As}$  and  $\alpha_{Cu/Pb}$ , shown in Fig. S10), which are much higher than 1. For competitive adsorption of Se(VI) and As(V), the values of  $\alpha_{Se/As}$  are in the same order of magnitude regardless of resin type, locating between 300 and 500 at pH 2. They all decrease to less than 50 when pH increases from 2 to 3. In terms of Cu(II) and Pb(II), no difference is found between the values of  $\alpha_{Cu/Pb}$  for 4 kinds of PEI-GA resins at pH 2. However, when pH increases to 2.5, the adsorption of Cu(II) increases dramatically, while that for Pb(II) remains almost the same, resulting in much higher  $\alpha_{Cu/Pb}$  values. Since PEI-GA1 and PEI-GA2 possess higher adsorption capacity for Cu(II), they present superior selectivity for Cu(II) over Pb(II) at this pH. As pH continues increasing to 3, these values decrease significantly as the adsorption capacity for Pb(II) starts growing up. To conclude, all the resins have a preference for Se(VI) over As(V) and Cu(II) over Pb(II). GA crosslinking hardly affects the preference for Se(VI), but it decreases the selectivity for Cu(II) over Pb(II) when pH is between 2.5 and 3.

The properties of the adsorbates (e.g., concentration, ionic size and

ionic charge, etc.) and the characteristics of the adsorbents (e.g., the structure and functional groups) are the factors affecting the different binding affinities for metals in multi-metal system. For Cu(II) and Pb(II) adsorption, based on Pearson's theory (Pearson, 1966), the hard acids prefer to associate with hard bases and soft acids prefer to associate with soft bases. Both Pb(II) and Cu(II) are considered as intermediate or borderline metal ions; the softness coefficients for Pb(II) is 0.41, very close to 0.38 for Cu(II) and the absolute hardness  $\eta_A$  of Pb(II) (8.5 eV) is slightly higher than that of Cu(II) (8.3 eV). Hence, the selective binding of Cu(II) over Pb(II) onto PEI-GA adsorbents should not be caused by the simple hard–soft concept. Therefore, the reason resulting in the selectivity is probably due to that copper, a transition element, is able to form more stable metal-ligand complexes compared to lead, a non-transition element (Atia et al., 2003); Cu(II) forms stable 4-coordinate square planar complexes with amines in aqueous solutions (Navarro et al., 1999), while Pb(II) prefers 4-coordinate octahedral complexes. The stability constant logarithm of metal-ammonia complexes is much higher for Cu(II) (4.12) than for Pb(II) (1.6) (Martell and Smith, 1974; Martin, 2002). These properties cause a poor adsorption performance of PEI-GA adsorbents for Pb(II); even in mono-metal system (Fig. S9, see SM), the adsorption capacity of PEI-GA1, PEI-GA2, PEI-GA3 and PEI-GA4 for Pb(II) at pH 3 is only 0.38, 0.28, 0.12 and 0.03 mmol g<sup>-1</sup>, respectively, much less than those for Cu(II). Such preference of Cu(II) adsorption onto GA crosslinked PEI can also be found in Cu(II)-Zn(II) binary system, where 4.5 wt% of Cu(II) was adsorbed, while almost no Zn(II) was adsorbed (Movahedi et al., 2015). The selectivity for Se(VI) over As(V) can be simply explained by the fact that at low pH (such as pH 2), As(V) existed mostly as H<sub>3</sub>AsO<sub>4</sub> (Fig. S5, See SM); with the increase of pH, the fraction of H<sub>2</sub>AsO<sub>4</sub><sup>-</sup> increases and competes with HSeO<sub>4</sub><sup>-</sup> and SeO<sub>4</sub><sup>2-</sup>. Briefly, under selected conditions, Cu(II) and Se(VI) can be successfully separated from Cu(II)-Pb(II) and Se(VI)-As(V) binary solutions, respectively, using PEI-GA resins, regardless of the amount of GA applied for crosslinking.

## 4. Conclusions

The amount of GA for PEI crosslinking does not affect the adsorption for selenate, especially when the PEI-GA ratio is less than 2. Moreover, the adsorption efficiency for Se(VI) is hardly affected by storage conditions; no significant difference can be observed between the freshly-prepared adsorbents and those stored in sealed or in open condition after 20 days. This can be explained by the fact that the adsorption of selenate occurs mainly through electrostatic attraction between selenate anions and protonated nitrogen. Thus it is only associated with N content and can be hardly affected by GA crosslinking or the reaction with CO<sub>2</sub>/H<sub>2</sub>O in the air. However, Cu(II) is adsorbed by chelation with free amine groups. The increase on GA amount reduces free primary amine groups on the adsorbents and thus decreases Cu(II) adsorption capacity. In addition, the adsorption capacity decreases significantly after 20-day storage in open condition due to the conversion of primary amine groups to carbamate when exposed to air. This loss of affinity can be recovered by thermal N<sub>2</sub> flow. The adsorbents could selectively recover Se(VI) from Se(VI)-As(V) system and Cu(II) from Pb(II)-Cu(II) system. The results of this study should be useful for the synthesis and storage of various PEI-based or amine-rich adsorbents applied for the removal of aqueous contaminants including anions and cations.

## Declaration of Competing Interest

The authors declare no conflict of interest.

## Acknowledgments

Y. Mo (CSC, Grant N° 201708450080) acknowledges the China Scholarship Council for providing PhD fellowship. Authors thank Jean-Claude Roux (IMT Mines Ales, C2MA) for his technical support for SEM

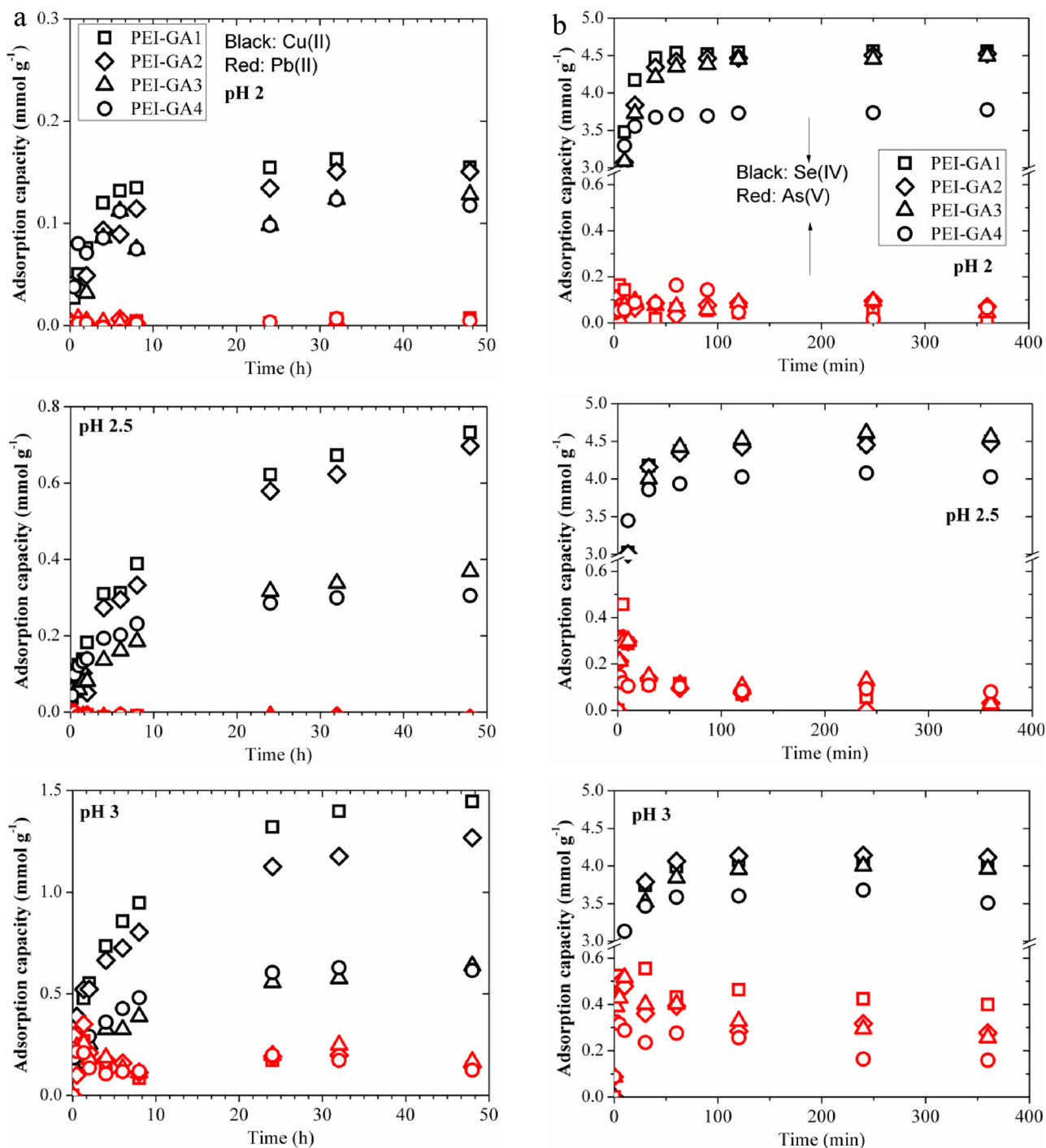


Fig. 7. Adsorption kinetics of (a) Se(VI) and As(V) and (b) Pb(II) and Cu(II) from binary solutions (Volume: 0.5 L; Room temperature; Adsorbent mass: 100 mg;  $C_0$ : 0.5 mmol L<sup>-1</sup> for Se(VI) and As(V) and 1 mmol L<sup>-1</sup> for Cu(II) and Pb(II)).

analyses. Authors are also thankful for the financial support of the National Natural Science Foundation of China (21777106) and the National Major Science and Technology Program for Water Pollution Control and Treatment (2017ZX07202).

#### Appendix A. Supplementary data

Supplementary material related to this article can be found, in the online version, at doi:<https://doi.org/10.1016/j.jhazmat.2019.121637>.

#### References

- An, B., Lee, H., Lee, S., Lee, S.-H., Choi, J.-W., 2015. Determining the selectivity of divalent metal cations for the carboxyl group of alginate hydrogel beads during competitive sorption. *J. Hazard. Mater.* 298, 11–18.
- Atia, A.A., Donia, A.M., Abou-El-Enein, S.A., Yousif, A.M., 2003. Studies on uptake behaviour of copper (II) and lead (II) by amine chelating resins with different textural properties. *Sep. Purif. Technol.* 33, 295–301.
- Bachvarova, A., Dimitriev, Y., Iordanova, R., 2005. Glass formation in the systems  $Ag_2SeO_3$ - $MnO_m$  and  $CuSeO_3$ - $MnO_m$  ( $MnO_m = B_2O_3, MoO_3$ ). *J. Non-cryst. Solids* 351, 998–1002.
- Baldwin, D.A., Betterton, E.A., Pratt, J.M., 1983. The chemistry of vitamin B 12. Part 22. Steric effects in the co-ordination of amines by cobalt (III) corrinoids. *J. Chem. Soc. Dalton Trans.* 2217–2222.

- Chou, Y.-H., Yu, J.-H., Liang, Y.-M., Wang, P.-J., Li, C.-W., Chen, S.-S., 2015. Recovery of Cu (II) by chemical reduction using sodium dithionite. *Chemosphere* 141, 183–188.
- Cotton, F.A., Wilkinson, G., 1988. *Advanced Inorganic Chemistry*. Wiley, New York.
- Erosa, M.D., Höll, W., Horst, J., 2009. Sorption of selenium species onto weakly basic anion exchangers: I. Equilibrium studies. *React. Funct. Polym.* 69, 576–585.
- Fukushi, K., Miyashita, S., Kasama, T., Takahashi, Y., Morodome, S., 2019. Superior removal of selenite by periclast during transformation to brucite under high-pH conditions. *J. Hazard. Mater.* 371, 370–380.
- Ghoul, M., Bacquet, M., Morcellet, M., 2003. Uptake of heavy metals from synthetic aqueous solutions using modified PEI–silica gels. *Water Res.* 37, 729–734.
- Hansen, H.K., Gutiérrez, C., Ferreiro, J., Rojo, A., 2015. Batch electro-dialytic treatment of copper smelter wastewater. *Miner. Eng.* 74, 60–63.
- Hansen, H.K., Peña, S.F., Gutiérrez, C., Lazo, A., Lazo, P., Ottosen, L.M., 2019. Selenium removal from petroleum refinery wastewater using an electrocoagulation technique. *J. Hazard. Mater.* 364, 78–81.
- Hu, D., Jiang, R., Wang, N., Xu, H., Wang, Y.-G., Ouyang, X., 2019. Adsorption of diclofenac sodium on bilayer amino-functionalized cellulose nanocrystals/chitosan composite. *J. Hazard. Mater.* 369, 483–493.
- Kaur, S., Kempson, I., Xu, H., Nydén, M., Larsson, M., 2018. Bio-template assisted synthesis of porous glutaraldehyde-polyethyleneimine particulate resin for selective copper ion binding and recovery. *RSC Adv.* 8, 12043–12052.
- Kiruba, R., Vinod, S., Zaibudeen, A., Solomon, R.V., Philip, J., 2018. Stability and rheological properties of hybrid  $\gamma$ -Al<sub>2</sub>O<sub>3</sub> nanofluids with cationic polyelectrolyte additives. *Colloids Surf. A Physicochem. Eng. Asp.* 555, 63–71.
- Kuila, T., Bose, S., Mishra, A.K., Khanra, P., Kim, N.H., Lee, J.H., 2012. Effect of functionalized graphene on the physical properties of linear low density polyethylene nanocomposites. *Polym. Test.* 31, 31–38.
- Kul, M., Oskay, K.O., 2015. Separation and recovery of valuable metals from real mix electroplating wastewater by solvent extraction. *Hydrometallurgy* 155, 153–160.
- Kwon, O.-H., Kim, J.-O., Cho, D.-W., Kumar, R., Baek, S.H., Kurade, M.B., Jeon, B.-H., 2016. Adsorption of As(III), As(V) and Cu(II) on zirconium oxide immobilized alginate beads in aqueous phase. *Chemosphere* 160, 126–133.
- Li, X., Wang, Z., Ning, J., Gao, M., Jiang, W., Zhou, Z., Li, G., 2018. Preparation and characterization of a novel polyethyleneimine cation-modified persimmon tannin bioadsorbent for anionic dye adsorption. *J. Environ. Manage.* 217, 305–314.
- Li, J., Yuan, S., Zhu, J., Van der Bruggen, B., 2019. High-flux, antibacterial composite membranes via polydopamine-assisted PEI-TiO<sub>2</sub>/Ag modification for dye removal. *Chem. Eng. J.* 373, 275–284.
- Lindén, J.B., Larsson, M., Kaur, S., Nosrati, A., Nydén, M., 2016. Glutaraldehyde-crosslinking for improved copper absorption selectivity and chemical stability of polyethyleneimine coatings. *J. Appl. Polym. Sci.* 133, 43954.
- Liu, C., Bai, R., San Ly, Q., 2008. Selective removal of copper and lead ions by diethylenetriamine-functionalized adsorbent: behaviors and mechanisms. *Water Res.* 42, 1511–1522.
- Ma, Y., Liu, W.-J., Zhang, N., Li, Y.-S., Jiang, H., Sheng, G.-P., 2014. Polyethyleneimine modified biochar adsorbent for hexavalent chromium removal from the aqueous solution. *Bioresour. Technol.* 169, 403–408.
- Martell, A.E., Smith, R.M., 1974. *Critical Stability Constants*. Springer.
- Martin, R.B., 2002. Practical hardness scales for metal ion complexes. *Inorg. Chim. Acta Rev.* 339, 27–33.
- Monier, M., Ayad, D., Wei, Y., Sarhan, A., 2010. Adsorption of Cu(II), Co(II), and Ni(II) ions by modified magnetic chitosan chelating resin. *J. Hazard. Mater.* 177, 962–970.
- Movahedi, A., Lundin, A., Kann, N., Nydén, M., Moth-Poulsen, K., 2015. Cu (I) stabilizing crosslinked polyethyleneimine. *Phys. Chem. Chem. Phys.* 17, 18327–18336.
- Navarro, R.R., Sumi, K., Matsumura, M., 1999. Improved metal affinity of chelating adsorbents through graft polymerization. *Water Res.* 33, 2037–2044.
- Pearson, R.G., 1966. *Acids and bases*. Science 151, 172–177.
- Ren, J., Musyoka, N.M., Langmi, H.W., North, B.C., Mathe, M., Pang, W., Wang, M., Walker, J., 2017. In-situ IR monitoring of the formation of Zr-fumarate MOF. *Appl. Surf. Sci.* 404, 263–267.
- Sanchez-Ballester, N.M., Soulaïrol, I., Bataille, B., Sharkawi, T., 2019. Flexible heteroionic calcium-magnesium alginate beads for controlled drug release. *Carbohydr. Polym.* 207, 224–229.
- Sharifi, M., Robatjazi, S.-M., Sadri, M., Mosaabadi, J.M., 2019. Immobilization of organophosphorus hydrolase enzyme by covalent attachment on modified cellulose microfibrils using different chemical activation strategies: characterization and stability studies. *Chin. J. Chem. Eng.* 27, 191–199.
- Sun, X.-F., Wang, S.-G., Cheng, W., Fan, M., Tian, B.-H., Gao, B.-Y., Li, X.-M., 2011. Enhancement of acidic dye biosorption capacity on poly(ethyleneimine) grafted anaerobic granular sludge. *J. Hazard. Mater.* 189, 27–33.
- Tabelin, C.B., Hashimoto, A., Igarashi, T., Yoneda, T., 2014. Leaching of boron, arsenic and selenium from sedimentary rocks: II. pH dependence, speciation and mechanisms of release. *Sci. Total Environ.* 473, 244–253.
- Vinodh, R., Abidov, A., Palanichamy, M., Cha, W.S., Jang, H.T., 2018. Constrained growth of solid amino alkyl siloxane (an organic–inorganic hybrid): the ultimate selective sorbent for CO<sub>2</sub>. *J. Ind. Eng. Chem.* 65, 156–166.
- Wang, S., Vincent, T., Faur, C., Rodríguez-Castellón, E., Guibal, E., 2019. A new method for incorporating polyethyleneimine (PEI) in algal beads: high stability as sorbent for palladium recovery and supported catalyst for nitrophenol hydrogenation. *Mater. Chem. Phys.* 221, 144–155.
- Wijesiri, R.P., Knowles, G.P., Yeasmin, H., Hoadley, A.F., Chaffee, A.L., 2019. CO<sub>2</sub> Capture from Air Using Pelletized Polyethyleneimine Impregnated MCF Silica. *Ind. Eng. Chem. Res.* 58, 3293–3303.
- Willner, I., Eichen, Y., Frank, A.J., Fox, M.A., 1993. Photoinduced electron-transfer processes using organized redox-functionalized bipyridinium-polyethyleneimine-titania colloids and particulate assemblies. *J. Phys. Chem.* 97, 7264–7271.
- Xu, X., Song, C., Andresen, J.M., Miller, B.G., Scaroni, A.W., 2002. Novel polyethyleneimine-modified mesoporous molecular sieve of MCM-41 type as high-capacity adsorbent for CO<sub>2</sub> capture. *Energy Fuel* 16, 1463–1469.
- Yamani, J.S., Lounsbury, A.W., Zimmerman, J.B., 2014. Adsorption of selenite and selenate by nanocrystalline aluminum oxide, neat and impregnated in chitosan beads. *Water Res.* 50, 373–381.
- Zhang, G., Zhao, P., Hao, L., Xu, Y., 2018. Amine-modified SBA-15 (P): a promising adsorbent for CO<sub>2</sub> capture. *J. CO<sub>2</sub> Util.* 24, 22–33.